PHYSICAL REVIEW B VOLUME 37, NUMBER 3 15 JANUARY 1988-II

Very large optical nonlinearity of semiconductor microcrystallites

Eiichi Hanamura
Department of Applied Physics, University of Tokyo, 7-3-1 Hongo, Bunkyo-ku, Tokyo 113, Japan
(Received 23 March 1987)

We analyze theoretically the oscillator strength and the third-order optical polarizability $\chi^{(3)}$ due to excitons in semiconductor microcrystallites. The nonlinear optical polarizability is shown to be greatly enhanced for an assembly of such microcrystallites as the exciton is quantized due to the confinement effect and the excitons in a single microcrystallite interact strongly enough to make the excitons deviate from ideal harmonic oscillators.

I. INTRODUCTION

Finite-size effects on optical properties have been observed for small colloidal CdS crystallites[1,2] and semiconductor microcrystallites embedded in a glass matrix.[3,4] On the other hand, zero- and one-dimensional semiconductor systems, which are called quantum-box and quantum-wire systems, are made artificially and studied extensively.[5] The electronic structure was also studied theoretically[6-8] and was shown to depend sensitively on the size of the microcrystallites relative to the electron and hole effective Bohr radii. From an engineering point of view, material with a large optical nonlinearity[9-11] is required for optical shutters or optical information processors.

In this paper we will discuss how to obtain very large oscillator strength and optical nonlinearity for an assembly of semiconductor boxes or spheres so small that the quantum confinement effect works in all three directions. The oscillator strength of the relevant optical transition increases with the size of the crystallite as long as the excited state is coherent. However, an exciton in a bulk crystal behaves almost as a harmonic oscillator which does not show any nonlinear optical response. Deviation of the electronic excitation from an ideal harmonic oscillator increases as the size of the microcrystallite decreases. As a result, we can imagine that there is an optimum size for obtaining the most effective optical nonlinearity. This will be clarified in this paper and it will also be shown how the radiative decay rate of the excitation depends on the size of the microcrystallite.

We derive the electronic structures of the excited states in a quantum box and quantum sphere of the semiconductor in Sec. II. The condition to obtain very large oscillator strength is presented in Sec. III together with the size-dependent decay rate of the excitation. It is discussed in Sec. IV how very large optical nonlinearity results from competition between the effect of large oscillator strength and the deviation of the exciton from an ideal boson. Discussion is given in Sec. V of how to observe these effects.

II. ELECTRONIC EXCITATION IN MICROCRYSTALLITE

There are several energies characterizing a microcrystallite. The first are size-quantization energies of electron ΔE_c and hole ΔE_v. The second is an average of the Coulomb attraction between an electron and a hole in the microcrystallite. This is denoted as the exciton energy V_{exc}. The third is the interaction energy V_{int} working between two excitations when they are formed in the microcrystallite. This characterizes the deviation of an excitation from an ideal boson. We have three limiting cases depending upon the relative sizes of the exciton energy and the quantization energy. Expressions are given for the electronic structures in these limits.

A. $V_{\text{exc}} \gg \Delta E_c, \Delta E_v$

In this limit the size quantization of the exciton is brought about. First, we consider a cubic box which contains N^3 unit cells. The electronic excited state is described by the Frenkel exciton as

$$\Psi_{\mathrm{n}} = \sum_{\mathrm{j}} F_{\mathrm{n}}(\mathrm{j}) W_{\mathrm{j}}^{c}(r_{\mathrm{j}}) \prod_{(\mathrm{i}\neq \mathrm{j})} W_{\mathrm{i}}^{v}(\mathbf{r}_{\mathrm{i}}) , \tag{1}$$

where W_{i}^{v} and W_{j}^{c} are Wannier functions of the valence and conduction bands, respectively, and $F_{\mathrm{n}}(\mathrm{j})$ is the envelope function in the quantum box:

$$F_{\mathrm{n}}(\mathrm{j}) = \left[\frac{2}{N}\right]^{3} \sin\left[\frac{\pi n_x j_x}{N}\right] \sin\left[\frac{\pi n_y j_y}{N}\right] \times \sin\left[\frac{\pi n_z j_z}{N}\right] . \tag{2}$$

The quantum number $\mathbf{n} = (n_x, n_y, n_z)$ and the site index $\mathrm{j} = (j_x, j_y, j_z)$ are chosen from positive integers between 1 and N. The ground state of the quantum box is given by

$$\Psi_g = \prod_{\mathrm{i}} W_{\mathrm{i}}^{v}(\mathbf{r}_{\mathrm{i}}) . \tag{3}$$

For the parabolic conduction and valence bands with effective masses m_e and m_h, respectively, the size quantization is governed by the relationship among the sample size $L = Nu$, and the effective Bohr radii of electron $a_e \equiv \hbar^2 \epsilon_0 / m_e e^2$ and hole $a_h \equiv \hbar^2 \epsilon_0 / m_h e^2$, where u is the length of the unit cell and ϵ_0 is the static dielectric constant. The size-quantization energies can be expressed for the electron and the hole, respectively, as follows:

$$\Delta E_c \equiv E_c(2,1,1) - E_c(1,1,1) = \frac{3\pi^2\hbar^2}{2m_e L^2} , \tag{4}$$

$$\Delta E_v \equiv E_v(2,1,1) - E_v(1,1,1) = \frac{3\pi^2\hbar^2}{2m_h L^2} . \tag{5}$$

The exciton energy V_{exc} is given by

$$V_{\text{exc}} = \frac{e^2}{\epsilon_0 a} = \frac{e^2}{\epsilon_0(a_e + a_h)} , \tag{6}$$

where a is an exciton Bohr radius. The condition (a) ($V_{\text{exc}} \gg \Delta E_c, \Delta E_v$), is equivalent to $V_{\text{exc}} \gg \Delta E_c + \Delta E_v$. This latter condition is rewritten in terms of Eqs. (4), (5), and (6) as

$$L \gg a_e + a_h = a . \tag{7}$$

The electronic excitation is expressed in this case as

$$\Psi_{\mathrm{n}} = \sum_{\mathrm{j}} \sum_{\mathrm{j}'} F_{\mathrm{n}}(\bar{\mathrm{j}}) \phi(\mathrm{j}_r) W_{\mathrm{j}}^c(\mathbf{r}_{\mathrm{j}}) \prod_{(\mathrm{i} \neq \mathrm{j}')} W_{\mathrm{i}}^v(\mathbf{r}_{\mathrm{i}}) , \tag{8}$$

where $\phi(\mathrm{j}_r)$ describes the electron-hole relative motion with $\mathrm{j}_r \equiv \mathrm{j} - \mathrm{j}'$ and $F_{\mathrm{n}}(\bar{\mathrm{j}})$ describes the center-of-mass motion of the exciton with $\bar{\mathrm{j}} \equiv (m_e \mathrm{j} + m_h \mathrm{j}')/(m_e + m_h)$. When the electron-hole relative motion is well localized at the same unit cell, $\phi(\mathrm{j}_r) = \delta_{\mathrm{jj}'}$, so that Eq. (8) is coincident with Eq. (1). On the other hand, the electronic excited state of the semiconductor microcrystallite can be described by the effective-mass approximation in terms of the Bloch functions $u_c(\mathbf{r})$ at the bottom of the conduction band and $u_v(\mathbf{r})$ at the top of the valence band. Then the center-of-mass motion and the electron-hole relative motion are approximated as

$$F_{\mathrm{n}}(\mathbf{R}) = \left[\frac{2}{L}\right]^3 \sin\left[\frac{\pi n_x R_x}{L}\right] \sin\left[\frac{\pi n_y R_y}{L}\right] \times \sin\left[\frac{\pi n_z R_z}{L}\right] , \tag{9}$$

$$\phi_{1s}(\mathbf{r}) = \left[\frac{1}{\pi a^3}\right]^{1/2} e^{-r/a} , \tag{10}$$

where $\mathbf{R} = u\bar{\mathrm{j}}$ and $\mathbf{r} = u(\mathrm{j} - \mathrm{j}')$.

Second, for the case of the quantum sphere with an infinite wall at $R \geq R_0$, the radius of the sphere, the envelope function of the center-of-mass motion, is given by

$$F_{nlm}(R,\theta,\varphi) = Y_{lm}(\theta,\varphi) \frac{\sqrt{2}}{R_0\sqrt{R}} \frac{J_{l+1/2}(k_{\ln}R)}{J_{l+3/2}(k_{\ln}R_0)} , \tag{11}$$

and that of the electron-hole relative motion is the same as Eq. (10). Here, Y_{lm} are the normalized spherical functions, $\hbar l$ is the momentum, $\hbar m$ is the projection of the momentum along a certain direction, and J_ν is a Bessel function. The quantities $k_{\ln}$ are given as solutions of the following equation:

$$J_{l+1/2}(k_{\ln}R_0) = 0 ,$$

where n is the serial number of the root of the Bessel function for a given value of l. In the case of $l = 0$, $k_{0n}R_0 = \pi n$ ($n = 1,2,\ldots$).

The energy of the exciton in the quantum box is

$$E_{\mathrm{n}} = E_g - E_{\text{exc}}^b + \frac{\hbar^2\pi^2\mathbf{n}^2}{2ML^2} ,$$

where $E_{\text{exc}}^b \equiv \mu e^4/2\hbar^2\epsilon_0^2$ is the exciton binding energy, $\mu = m_e m_h/(m_e + m_h)$, $M = m_e + m_h$, and $\mathbf{n} = (n_x, n_y, n_z)$ with $n_x, n_y, n_z \geq 1$. The energy of the optically allowed exciton with $l = m = 0$ in the quantum sphere is similarly given for $n \geq 1$ by

$$E_{n00} = E_g - E_{\text{exc}}^b + \frac{\hbar^2\pi^2 n^2}{2MR_0^2} .$$

B. $V_{\text{exc}} \ll \Delta E_c, \Delta E_v$

This is opposite to the case (a), and is equivalent to the condition $L \ll \min(a_e, a_h)$. Here the size-quantization effect of the electron and the hole is much larger than the exciton effect so that the latter effect is neglected. Then the wave function of the excited state is given by

$$\Psi_{\mathrm{mn}} = \sum_{\mathrm{j}} \sum_{\mathrm{j}'} F_{\mathbf{m}}^c(\mathrm{j}) F_{\mathrm{n}}^v(\mathrm{j}') W_{\mathrm{j}}^c(\mathbf{r}_{\mathrm{j}}) \prod_{(\mathrm{i} \neq \mathrm{j}')} \mathrm{W}_{\mathrm{i}}^{\mathrm{v}}(\mathbf{r}_{\mathrm{i}}) , \tag{12}$$

where $F_{\mathbf{m}}^c(\mathrm{j})$ and $F_{\mathrm{n}}^v(\mathrm{j}')$ are envelope functions of the conduction-band electron and the valence-band hole, respectively, and have the same form as Eq. (2) for the quantum box. In the case of the quantum sphere, $F_{\mathbf{m}}^c(\mathbf{r})$ and $F_{\mathbf{n}}^v(\mathbf{r}')$ have the same forms as Eq. (11) with $\mathbf{m} = (n,l,m)$, $\mathbf{n} = (n',l',m')$ but here $\mathbf{r} = u\,\mathrm{j}$ and $\mathbf{r}' = u\,\mathrm{j}'$ are the electron and hole coordinates treated as continuous variables. The optical transition is allowed only between the conduction and valence band states with the same quantum numbers $\mathbf{m} = \mathbf{n}$. This excitation energy for $\mathbf{m} = \mathbf{n}$, is given as

$$E_{\mathrm{n}} = E_g + \frac{\hbar^2\pi^2}{2\mu L^2}(n_x^2 + n_y^2 + n_z^2) \tag{13}$$

for the quantum box and

$$E_{nml} = E_g + \frac{\hbar^2}{2\mu} k_{\ln}^2 \tag{14}$$

for the quantum sphere.

C. $\Delta E_c \gg V_{\text{exc}} \gg \Delta E_v$

This condition is rewritten in terms of the effective Bohr radii as follows:

$$a_e \gg L, R_0 \gg \sqrt{a_h a} > a_h .$$

First, the most dominant kinetic energy of the electron is quantized due to the confinement effect. Then we have the same expression for the electron states in the quantum box and sphere, respectively, as Eqs. (1) and (11) in the zeroth-order approximation. Here $F_{\mathrm{n}}(\mathrm{j})$ and $F_{nlm}(\mathbf{r})$ denote the electron envelope functions, respectively, in the quantum box and sphere. Second, when the electron-hole Coulomb interaction is taken into account, the hole is well localized in the central part of the microcrystallite as shown for the quantum sphere in the following.

Taking into account the inequality (c), we may assume the following wave function for the electron and hole in the quantum sphere with the radius $R_0 \equiv \mu N$:

$$\Psi_{nlm}^{n'l'm'}(\mathbf{r}_e,\mathbf{r}_h) = F_{nlm}(\mathbf{r}_e)\chi_{nlm}^{n'l'm'}(\mathbf{r}_h) \; .$$

When the electron is in the state (n, $l=0$, $m=0$), the hole experiences a spherical symmetric potential

$$V_{n00} = -\frac{e^2}{\epsilon_0}\int \frac{|\Psi_{n00}(\mathbf{r}')|^2}{|\mathbf{r}-\mathbf{r}'|}d\mathbf{r}' = -\frac{e^2}{\epsilon_0 R_0}\beta_n + \tfrac{1}{2}m_h\omega_n^2 r^2 \; , \tag{15}$$

where

$$\beta_n = 2\int_0^{n\pi}\frac{\sin^2 y}{y}dy \; ,$$

$$\omega_n^2 = \frac{2}{3}\frac{\pi^2 n^2}{m_h R_0^2}\frac{e^2}{\epsilon_0 R_0} \; .$$

The effective-mass equation for $\chi_{n00}^{n'00}$ is solved with the potential (15) as

$$\chi_{n00}^{n'00}(r) = \left[\frac{m_h\omega_n}{\pi\hbar}\right]^{1/4}\frac{1}{\sqrt{2^{n'}n'!}}\exp\left[\frac{-m_h\omega_n}{2\hbar}r^2\right] \times \frac{H_{n'}\left[r\left[\frac{m_h\omega_n}{\hbar}\right]^{1/2}\right]}{r} \; , \tag{16}$$

$$E_{n00}^{n'00} = E_g - \frac{e^2}{\epsilon_0 a}\beta_n + \hbar\omega_n(n'+\tfrac{1}{2}) \quad (n,n' \geq 1) \; , \tag{17}$$

where $H_{n'}$ is the n'th order Hermite polynomial.

Under case (a), $L, R_0 \gg a_e + a_h = a$, the center-of-mass motion of the exciton is quantized due to the quantum confinement of the exciton while for case (b), $L, R_0 \ll a_e, a_h$, both the electron and the hole motions are quantized independently. Under case (c), $a_e \gg L$, $R_0 \gg a_h$, the electron motion is quantized and the hole is trapped through the Coulomb potential of the electron quantized inside the quantum dot.

III. OSCILLATOR STRENGTH IN QUANTUM DOT

The size-quantization effect on the absorption spectrum was observed[1,2] and theoretically studied already[3,4]. We find that the effect of very large oscillator strength is brought about in case (a) but not in case (b). Case (c) is marginal. Because of the sum rule, however, the sum of the whole oscillator strength is constant in all the cases as long as the concentration of the optical-active medium is kept constant. Therefore the oscillator strength is concentrated in the lower excitations in case (a), as will be shown.

A. $V_{\text{exc}} \gg \Delta E_c, \Delta E_v$

The transition dipole moment to these excited states Ψ_{n} from the ground state Ψ_g is evaluated for the Frenkel exciton in case (a) as follows:

$$\langle \Psi_{\text{n}} | P | \Psi_g \rangle = \sum_{\text{j}} F_{\text{n}}(\text{j})\langle W_{\text{j}}^c(\mathbf{r}_{\text{j}}) | p_{\text{j}} | W_{\text{j}}^v(\mathbf{r}_{\text{j}})\rangle = p_{\text{cv}}\left[\frac{2}{N}\right]^{2/3}\cot\left[\frac{\pi n_x}{2N}\right]\cot\left[\frac{\pi n_y}{2N}\right] \times \cot\left[\frac{\pi n_z}{2N}\right] \; , \tag{18}$$

where P is a component of the dipole-moment operator $\mathbf{P}$:

$$\mathbf{P} = \sum_i \mathbf{p}_i$$

and $\langle W_{\text{j}'}^c(\mathbf{r}_{\text{j}}) | p_{\text{j}} | W_{\text{j}}^v(\mathbf{r}_{\text{j}})\rangle = p_{cv}\delta_{\text{jj}'}$. The transition dipole moment to the lowest excited state $(n_x, n_y, n_z) = (1,1,1)$ is given in good approximation as follows:

$$\langle \Psi_{111} | P | \Psi_g \rangle = \left[\frac{2\sqrt{2}}{\pi}\right]^3 p_{cv}N^{3/2} \; . \tag{19}$$

For the transition to such a low excited state (n_x, n_y, n_z) as $n_{x,y,z} \ll N$.

$$\langle \Psi_{\text{n}} | P | \Psi_g \rangle = \left[\frac{2\sqrt{2}}{\pi}\right]^3 p_{cv}N^{3/2}/(n_x n_y n_z) \; . \tag{20}$$

Then the oscillator strength f_{n} per quantum box is given by

$$f_{\text{n}} = \frac{2m}{\hbar}\omega_{\text{n}}|p_{cv}|^2\left[\frac{2\sqrt{2}}{\pi}\right]^6\frac{N^3}{(n_x n_y n_z)^2} \; . \tag{21}$$

For the Wannier exciton in the quantum box, the envelop function is described by Eqs. (9) and (10), and the oscillator strength is obtained by multiplying Eq. (21) by $u^3|\phi_{1s}(0)|^2 = u^3/(\pi a^3)$ for the lowest exciton. Here the excitation is a coherent state over the whole quantum box in case (a). The factor N^3 in Eq. (21) comes from this coherency. It is noted from Eq. (21) that the oscillator strengths are concentrated on the low excited states. The concentration of the quantum boxes per unit volume is made equal to $1/L^3$ so that the oscillator strength per unit volume is naturally independent of N^3.

The transition dipole moment to the excited state (n, $l=0$, $m=0$) for the quantum sphere is given by

$$\int d\mathbf{R}\Psi_{n00}(\mathbf{R})\phi_{1s}(0)p_{cv} = p_{cv}\phi_{1s}(0)2\sqrt{2/\pi}\frac{1}{n}R_0^{3/2} \; . \tag{22}$$

As a result, the oscillator strength for $R_0 \equiv uN$ is

$$f_{n00} = \frac{2m}{\hbar}\omega_n|p_{cv}\phi_{1s}(0)|^2 u^3\left[2\left[\frac{2}{\pi}\right]^{1/2}\right]^2\frac{N^3}{n^2} \; . \tag{23}$$

For the quantum sphere with the radius $R_0 \equiv uN$, we have the same N dependence of the oscillator strength as for the quantum box with $L = uN$. Only a numerical factor is different.

B. $\Delta E_c, \Delta E_v \gg V_{\text{exc}}$

The transition dipole moment for the quantum box under condition (b) is in contrast to case (a) as follows:

$$\begin{aligned}\langle \Psi_{\mathrm{mn}} \mid P \mid \Psi_g \rangle &= \sum_{\mathrm{j}} \sum_{\mathrm{j}'} F_{c\mathrm{m}}(\mathrm{j}) F_{v\mathrm{n}}(\mathrm{j}') \\ &\qquad \times \langle W_{\mathrm{j}}^{c}(\mathbf{r}_{\mathrm{j}}) \mid p_{\mathrm{j}'} \mid W_{\mathrm{j}'}^{v}(\mathbf{r}_{\mathrm{j}'}) \rangle \\ &= \sum_{\mathrm{j}} \sum_{\mathrm{j}'} F_{c\mathrm{m}}(\mathrm{j}) F_{v\mathrm{n}}(\mathrm{j}') p_{cv} \delta_{\mathrm{jj}'} \\ &= p_{cv} \delta_{\mathrm{mn}} \ . \end{aligned} \tag{24}$$

For the quantum sphere,

$$\begin{aligned}\langle \Psi_{nlm}^{n'l'm'} \mid P \mid \Psi_g \rangle &= p_{cv} \int F_{nlm}(\mathbf{r}) F_{n'l'm'}(\mathbf{r}) d\mathbf{r} \\ &= p_{cv} \delta_{nn'} \delta_{ll'} \delta_{mm'} \ . \end{aligned} \tag{25}$$

These results mean that the interband optical transition between the conduction- and valence-band states with the same quantum numbers is allowed and that the value of the transition dipole moment is independent of the quantum number n or (nlm) for all the allowed transitions.

Therefore the sum of all the oscillator strengths per unit volume becomes also naturally independent of the size of the microcrystallite in both cases (a) and (b). Contrary to these absorption spectra, we have the size dependences of the radiative decay rate and the nonlinear optical response only for case (a).

The radiative decay rate is proportional to the oscillator strength. As a result, the exciton decay rate in case (a) is proportional to the number of unit cells in the box volume N^3 while it is independent of N^3 in case (b). This originates from the same effect as the very large oscillator strength of the bound exciton. Nobody has observed this effect yet. The conditions for observing this effect will be discussed later.

C. $\Delta E_c \gg V_{\text{exc}} \gg \Delta E_v$

Transition dipole moment of the quantum sphere is evaluated in terms of Eqs. (11) and (16) as follows:

$$\begin{aligned}\langle \Psi_{n00}^{n'00} \mid P \mid \Psi_g \rangle &= p_{cv} \int \Psi_{n00}(\mathbf{R}) \chi_{n00}^{n'00}(\mathbf{R}) d\mathbf{R} \\ &= p_{cv} \left[\frac{\hbar}{m_h \omega_n} \right]^{1/2} \int_0^{R_0 \left[\frac{m_h \omega_n}{\hbar} \right]^{1/2}} \sin \left[\frac{n\pi}{R_0} \left[\frac{\hbar}{m_h \omega_n} \right]^{1/2} y \right] \exp(-\tfrac{1}{2} y^2) H_{n'}(y) dy \\ &= p_{cv} \left[\frac{\hbar}{m_h \omega_n} \right]^{1/2} (-1)^m \sqrt{\pi/2}\, \beta^{2m+1} \exp(-\tfrac{1}{2}\beta^2) \ , \end{aligned} \tag{26}$$

where $\beta \equiv (n\pi/R_0)(\hbar/m_h\omega_n)^{1/2}$, $n' \equiv 2m+1$ and $R_0\sqrt{m_h\omega_h/\hbar}$ was approximated as ∞ in the upper limit of the integral. The oscillator strength of the lowest excitation ($n=1$, $n'=1$) has a much weaker enhancement of the oscillator strength [$\sim N \exp(-\alpha/\sqrt{N}\,)$ with $\alpha \equiv \sqrt{3\pi a_h/8u}$] than in case (a).

IV. VERY LARGE OPTICAL NONLINEARITY

We will show very large nonlinear optical polarizability which depends on the size of the microcrystallite. This enhancement originates from two conflicting concepts. One is due to the size quantization of excitons. The oscillator strength concentrates on the lowest coherent excited state in case (a). This results in an enhancement factor of L^6 for the third-order nonlinear optical polarizability $\chi^{(3)}(\omega; -\omega, \omega, -\omega)$ per microcrystallite, i.e., the enhancement factor L^3 for $\chi^{(3)}$ per unit volume. The other enhancement comes from deviation of the electronic excitation from an ideal harmonic oscillator. When the size of the microcrystallite is reduced, the latter effect increases while the former decreases. The third-order optical polarization is evaluated as

$$\langle P^{(3)}(\mathbf{r},t) \rangle = \left[\frac{-i}{\hbar} \right]^3 \int_{-\infty}^{t} dt_1 \int_{-\infty}^{t_1} dt_2 \int_{-\infty}^{t_2} dt_3 \langle P(r,t)[H'(t_1),[H'(t_2),[H'(t_3),\rho_0]]] \ . \tag{27}$$

The integrand is composed of the following eight terms:

$$\langle P(t) H'(t_1) H'(t_2) H'(t_3) \rho_0 \rangle \ , \tag{28a}$$

$$-\langle H'(t_2) H'(t_3) \rho_0 H'(t_1) P(t) \rangle \ , \tag{28b}$$

$$-\langle H'(t_1) H'(t_3) \rho_0 H'(t_2) P(t) \rangle \ , \tag{28c}$$

$$+\langle P(t) H'(t_3) \rho_0 H'(t_2) H'(t_1) \rangle \ , \tag{28d}$$

$$-\langle H'(t_1) H'(t_2) \rho_0 H'(t_3) P(t) \rangle \ , \tag{28e}$$

$$+\langle P(t) H'(t_2) \rho_0 H'(t_3) H'(t_1) \rangle \ , \tag{28f}$$

$$+\langle P(t) H'(t_1) \rho_0 H'(t_3) H'(t_2) \rangle \ , \tag{28g}$$

$$-\langle \rho_0 H'(t_3) H'(t_2) H'(t_1) P(t) \rangle \ . \tag{28h}$$

Here we consider only the resonant case in which the energy of the incident photon $\hbar\omega$ is nearly equal to the first excitation energy $\hbar\omega_0$, and neglect contribution to the nonlinear polarization from the other levels and the antiresonant components. The contribution of each term in Eqs. (16) to the degenerate four-wave mixing through $P^{(3)}$ is presented[12] by the Feynman diagrams in Fig. 1. Then, e.g., the first term of Eq. (28a) has two contributions:

$$\langle 0|P(t)|1\rangle\langle 1|H'(t_1)|0\rangle\langle 0|H'(t_2)|1\rangle \times\langle 1|H'(t_3)|0\rangle ,$$

$$\langle 0|P(t)|1\rangle\langle 1|H'(t_1)|2\rangle\langle 2|H'(t_2)|1\rangle \times\langle 1|H'(t_3)|0\rangle .$$

These correspond, respectively, to diagram (1) $|0\rangle\langle 0|$ and (1) $|2\rangle\langle 2|$ in Fig. 1. We denote the ground state, the excited states with an excitation and with two excitations, respectively, by $|0\rangle$, $|1\rangle$, and $|2\rangle$. Here we assume the amplitude of the excited state to decay with a decay constant γ.

Note that both the left- and right-hand side propagating states in the density operator are in the ground states for the time interval between t_1 and t_2 in the diagrams of (1) $|0\rangle\langle 0|$, (2), (7), and (8) $|0\rangle\langle 0|$ in Fig. 1. Therefore these contributions to $P^{(3)}$ are canceled out by those coming from the renormalization of the ground state. As a result, we must pick up the connected diagrams (1) $|2\rangle\langle 2|$, (4), and (6) in Fig. 1 for the emission process $\chi^{(2)}(\omega;-\omega,\omega,-\omega)$. Diagrams (3), (5), and (8) $|2\rangle\langle 2|$ contribute to the third-order process of the photon absorption $\chi^{(3)}(-\omega;\omega,-\omega,\omega)$. Here the electric field E was assumed to be almost constant inside the quantum microcrystallite. Then we have the following expression for $\chi^{(3)}(\omega;-\omega,\omega,-\omega)$ per a single microcrystallite:

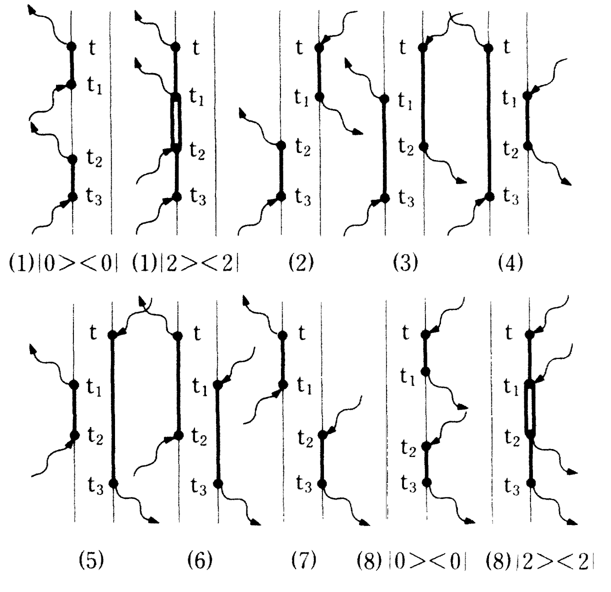

FIG. 1. The Feynman diagrams of third-order optical polarization under near resonant condition of exciton. Single and double solid lines describe the propagation, respectively, of a single exciton and of two excitons in a microcrystallite, and thin lines that of the electronic ground state.

$$\chi^{(3)}=\frac{|P|^4}{\hbar^3(\omega-\omega_0+i\Gamma)^2(\omega-\omega_0-i\Gamma)}\frac{\gamma'}{\gamma}+\frac{|P|^4(\omega_{\text{int}}-2i\Gamma)}{\hbar^3(\omega-\omega_0+i\Gamma)^2(\omega-\omega_0-i\Gamma)(\omega_0-\omega+\omega_{\text{int}}-i\Gamma)} . \tag{29}$$

Here $\Gamma=\gamma+\gamma'$ is the transverse relaxation rate, γ', the phase relaxation rate, and 2γ the decay rate of the exciton. $\hbar\omega_{\text{int}}\equiv V_{\text{int}}$ denotes the interaction energy of two excitons in the microcrystallite. When the exciton interaction $\hbar\omega_{\text{int}}$ and all the relaxation rates are negligible in comparison with the off-resonance energy $|\omega-\omega_0|$, $\chi^{(3)}(\omega;-\omega,\omega,-\omega)$ vanishes. Under such a condition, excitons behave as harmonic oscillators, which do not show any nonlinear response. Under such an opposite condition as $\omega_{\text{int}}>|\omega-\omega_0|$, we have the enhanced optical nonlinearity shown in the following, which comes from the second term of Eq. (29). As to the first term, the enhancement of $|P|^4$ is partially compensated by the radiative decay rate 2γ in the denominator as will be discussed in Sec. V. The third-order optical polarizability $\chi^{(3)}_{\text{box}}$ for such a microcrystallite as the interaction energy between two excitations becomes larger than the off-resonance energy is given by

$$\chi^{(3)}_{\text{box}}=\left[\frac{2\sqrt{2}}{\pi}\right]^{12}\frac{|p_{cv}|^4}{\hbar^3(\omega-\omega_0)^3}N^6 , \tag{30a}$$

where we used the transition dipole moment for case (a) given by Eq. (9). $\chi^{(3)}$ per unit volume is

$$\chi^{(3)}=\left[\frac{2\sqrt{2}}{\pi}\right]^{12}\frac{|p_{cv}|^4}{\hbar^3(\omega-\omega_0)^3u^3}N^3 . \tag{30b}$$

Here we assumed close-packed quantum boxes, the concentration of which is $N_c=L^{-3}=(uN)^{-3}$. For the Wannier exciton in the box, p_{cv} should be replaced by $p_{cv}\phi(0)u^{3/2}$ in Eqs. (30a) and (30b), where $\phi(0)$ is the amplitude at the origin of the electron-hole relative motion. For the Wannier exciton in the quantum sphere, we have the nonlinear optical polarizability $\chi^{(3)}$ similar to Eqs. (30a) and (30b) with different numerical factors:

$$\chi^{(3)}_{\text{sphere}}=\left[2\left[\frac{2}{\pi}\right]^{1/2}\right]^4\frac{|p_{cv}|^4|\phi(0)|^4u^6}{\hbar^3(\omega-\omega_0)^3}N^6 , \tag{31a}$$

and $\chi^{(3)}$ per unit volume is

$$\chi^{(3)}=\left[2\left[\frac{2}{\pi}\right]^{1/2}\right]^4\frac{|p_{cv}|^4|\phi(0)|^4u^3}{\hbar^3(\omega-\omega_0)^3}N^3 . \tag{31b}$$

For case (b), the transition dipole moment is independent of the quantum number n so that $\chi^{(3)}_{\text{box}}$ per a quantum box is

$$\chi^{(3)}_{\rm box}=\sum_{\rm n}\frac{|p_{cv}|^4}{\hbar^3(\omega-\omega_{\rm n})^3}\ . \tag{32}$$

Here we have the same expression for $\chi^{(3)}_{\rm sphere}$ per a quantum sphere. For such an off-resonant case as $|\omega-\omega_{111}| \gg |\omega_{\rm NNN}-\omega_{111}|$, the denominator of Eq. (32) is replaced by an average value $(\omega-\bar{\omega})^3$ and $\chi^{(3)}$ per unit volume becomes independent of N as

$$\chi^{(3)}=\frac{|p_{cv}|^4}{\hbar^3(\omega-\bar{\omega})^3}N^3\frac{r}{N^3u^3}$$

$$=\frac{|p_{cv}|^4 r}{\hbar^3(\omega-\bar{\omega})^3u^3}\ ,$$

where r is a volume fraction of the optically active material. As a result, we have the very large enhancement N^3 of $\chi^{(3)}$ only for case (a). When the excited state is expressed by Eq. (8), the squared transition dipole moment $|P|^2$ is reduced by the factor $u^3/(\pi a^3)$. This comes from the fact that the Wannier exciton is formed by a superposition of the Bloch states inside the sphere with a radius $(1/a)$ in the Brillouin zone. This is in contrast with the case of a Frenkel exciton which has no such reduction factor.

V. OBSERVATION OF ENHANCED OPTICAL NONLINEARITY

Let us discuss the limitations for realizing very large optical nonlinearity. First, the conditions for case (a) must be satisfied so that

$$\frac{e^2}{\epsilon_0 a} \gg \Delta E_c, \Delta E_v\ .$$

Here the energy separations of the conduction and valence bands in the quantum box are given by Eqs. (4) and (5), and for the quantum sphere,

$$\Delta E_c \equiv E_c(200)-E_c(100)=\frac{3\pi^2\hbar^2}{2m_eR_0^2}\ ,$$

$$\Delta E_v \equiv E_v(200)-E_v(100)=\frac{3\pi^2\hbar^2}{2m_hR_0^2}\ ,$$

where the arguments represent (n,l,m). Second, the single lowest excited state is required to be dominant in $\chi^{(3)}$ so that

$$\hbar|\omega-\omega_0| \ll \frac{3\pi^2\hbar^2}{2(m_e+m_h)}\left[\frac{1}{L^2}\ \text{or}\ \frac{1}{R_0^2}\right]\ ,$$

where the right-hand side denotes a quantization energy of the center-of-mass motion of the exciton in the quantum box or sphere. Third, in order to get enough deviation of excitation from an ideal harmonic oscillator, the interaction energy between two excitons[13]

$$V_{\rm int}=8\pi E^b_{\rm exc}\frac{m_em_h}{(m_e+m_h)^2}\frac{a^2f_0}{L^3}$$

for the quantum box and

$$V_{\rm int}=6E^b_{\rm exc}\frac{m_em_h}{(m_e+m_h)^2}\frac{a^2f_0}{R_0^3}$$

for the quantum sphere should be larger than the off-resonant energy, where $E^b_{\rm exc}$ is the exciton binding energy and f_0 is the scattering amplitude. f_0 is equal to $3.3a$ for excitons in CuCl.[13] The phase relaxation in the electronic excitation γ' also has an effect which makes the excitonic excitations deviate from ideal harmonic oscillators. The third-order optical polarizability was derived,[12] taking into account the phase relaxation γ' in the single excited state and the interaction between two excitons in the double excited state, as shown by Eq. (29).

Here we have considered that the second excitation in the microcrystallite has the energy $\hbar\omega_0+V_{\rm int}$. First we see from Eq. (29) that $\chi^{(3)}$ becomes finite when $V_{\rm int}$ is of the same order as or larger than the off-resonance energy $\hbar|\omega_0-\omega|$. Second, as far as phase relaxation occurs $\chi^{(3)}$ is enhanced by the factor (γ'/γ) in addition to the enhanced-oscillator-strength effect through the factor $|P|^4$. However, the radiative decay rate 2γ is also enhanced by the effect of the enhanced oscillator strength in case (a):

$$2\gamma=2\gamma_0AN^3\ ,$$

where $2\gamma_0$ is the radiative decay rate of the bulk exciton, $A=(2\sqrt{2/\pi})^{12}$ for the quantum box, and $A=(2\sqrt{2/\pi})^4$ for the quantum sphere. On the other hand, the concentration N_c of the boxes and the spheres are, respectively, $N_c=1/L^3$ for the full-packed quantum boxes with the side length $L=uN$, and $N_c=3r/4\pi R_0^3$ for the quantum spheres with the molecular concentration r, e.g., semiconductor spheres in glass or colloidal particles of the semiconductor with the radius $R_0=uN$. As a result, the first term of Eq. (29) becomes independent of N and loses the enhancement due to the very large oscillator strength.

We conclude that only when $V_{\rm int}$ becomes nearly equal to or larger than the off-resonance energy $\hbar|\omega_0-\omega|$, does enhancement of $\chi^{(3)}$ due to very large oscillator strength occur effectively through the second term of Eq. (29). Summarizing the conditions for enhanced $\chi^{(3)}$, N should satisfy the following inequalities:

$$\left[\frac{\epsilon_0 aE_v'}{e^2}\right]^{1/2}\left[\frac{\epsilon_0 aE_c'}{e^2}\right]^{1/2} \ll N$$

$$< \min\left[\left[\frac{E'_{\rm exc}}{\hbar|\omega-\omega_0|}\right]^{1/2},\ \left[\frac{8\pi E^b_{\rm exc}a^2f_0m_em_h}{\hbar|\omega-\omega_0|u^3(m_e+m_h)^2}\right]^{1/3}\right]\ , \tag{33}$$

where $E'_{\text{exc}} \equiv 3\pi^2\hbar^2/2(m_e+m_h)u^2$, $E'_c \equiv 3\pi^2\hbar^2/2m_e u^2$, and $E'_v \equiv 3\pi^2\hbar^2/2m_h u^2$.

When we use the numerical values for the CuCl crystal $\epsilon_0=5.1$, $u=3.2$ Å, $a=6.6$ Å, $E^b_{\text{exc}}=0.2$ eV, $m_e=0.5m$, and $m_h=2.0m$, and choose the off-resonance energy $\hbar|\omega-\omega_0|=5$ meV, the condition (33) is $2 \ll N < 20$. When we choose $N=20$, i.e., $L=64$ Å, we can expect enhancement of an order of 10^4 for $\chi^{(3)}$. If we choose the situation of CdS and CdSe $\epsilon_0=8.5$, $u=3.5$ Å, $a=30$ Å, $E^b_{\text{exec}}=30$ meV, $m_e=0.25m$, $m_h=1.6m$ ($m_{h\perp}=0.7m$, $m_{h\parallel}=5m$), and $\hbar|\omega-\omega_0|=10$ meV, we cannot find any N which satisfy Eq. (33). $(\epsilon_0 a E'_c/e^2)^{1/2}$ is 31 while $(E'_{\text{exc}}/\hbar|\omega-\omega_0|)^{1/2}$ is 27 and $[(8\pi E^b_{\text{exc}} a^2 f_0 \mu)/(\hbar|\omega-\omega_0|u^3 M)]^{1/3}$ is 26. However, the enhanced-oscillator-strength effect works partially even for $N \sim 30$ corresponding to $R_0 \sim 100$ Å. Third-order optical processes were observed in semiconductor-doped glasses.[14–16] Jain and Lind observed[14] $\chi^{(3)} \sim 1.3\times10^{-8}$ esu for the color filter of $\text{CdS}_{0.9}\text{Se}_{0.1}$ in glass and $\chi^{(3)} \sim 3.4\times10^{-9}$ esu for bulk CdS using light with wavelength 0.53 μm. The mole concentration of $\text{CdS}_{0.9}Se_{0.1}$ in glass is estimated to be 1% so that we have have an enhancement of 400 of $\chi^{(3)}$ for the close-packed quantum spheres. We need a more elaborate calculation to evaluate the enhancement quantitatively for the region in which the inequalities (33) are not satisfied. The size of the semiconductor spheres doped in glass has dispersion. This also makes the theoretical comparison difficult.

The very large optical nonlinearity presented in this paper cannot be expected for microcrystallites of GaAs and other III-V semiconductors. These have rather lighter effective masses of electron and hole and larger dielectric constant than in I-VII and II-VI semiconductors. As a result, the quantization energies of electron and hole become easily larger than the exciton binding energy so that the conditions of Eq. (33) are not satisfied. In these materials, the band-filling effect and the screening effects due to the free carriers appear dominant under strong pumping as discussed in Refs. 8 and 11. The present enhancement of $\chi^{(3)}$ due to the exciton quantization is expected only for microcrystallites made of materials with the larger binding energy and the smaller effective Bohr radius of excitons such as I-VII and II-VI semiconductors, and only for such a low temperature as $k_B T \ll E^b_{\text{exc}}$.

ACKNOWLEDGMENTS

This work was partially supported by the Scientific Research Grant-in-Aid No. 61214003 for Special Project Research on "Alloy Semiconductor Physics and Electronics," from the Japanese Ministry of Education, Science, and Culture.

---

[1] R. Rossetti, S. Nakahara, and L. E. Brus, J. Chem. Phys. **79**, 1086 (1983).

[2] R. Rossetti, J. L. Ellison, J. M. Gibson, and L. E. Brus, J. Chem. Phys. **80**, 4464 (1984).

[3] A. I. Ekimov, Al. L. Efros, and A. A. Onuschchenko, Solid State Commun. **56**, 921 (1985).

[4] J. Warnoch and D. D. Awschalom, Phys. Rev. B **32**, 5529 (1985).

[5] Y. Arakawa and H. Sakaki, Appl. Phys. Lett. **40**, 939 (1982); A. B. Fowler, A. Hartstein, and R. A. Webb, Phys. Rev. Lett. **48**, 196 (1982); W. J. Skocpol, L. D. Jackel, E. L. Hu, R. E. Howard, and L. A. Fetter, *ibid.* **49**, 951 (1982); P. M. Petroff, A. C. Gossard, R. A. Logan, and W. Wiegmann, Appl. Phys. Lett. **41**, 635 (1982); K. Kash, A. Scherer, J. M. Worlock, H. G. Craighead, and M. C. Tamargo, *ibid.* **49**, 1043 (1986); J. Cibert, P. M. Petroff, G. L. Dolan, S. J. Pearton, A. C. Gossard, and J. H. English, *ibid.* **49**, 1275 (1986); Y. Miyamoto, M. Cao, Y. Shingai, K. Furuya, Y. Suematsu, K. G. Ravikumar, and S. Arai, Jpn. J. Appl. Phys. **26**, L225 (1987).

[6] Al. L. Efros and A. L. Efros, Fiz. Tekh. Poluprovodn. **16**, 1209 (1982) [Sov. Phys.—Semicond. **16**, 772 (1982)].

[7] L. E. Brus, J. Chem. Phys. **79**, 5566 (1983); **80**, 4403 (1984).

[8] S. Schmitt-Rink, D. A. B. Miller, and D. S. Chemla, Phys. Rev. B **35**, 8113 (1987).

[9] M. Dagenais and W. F. Sharfin, J. Opt. Soc. Am. B **2**, 1179 (1985).

[10] T. Takagahara and E. Hanamura, Phys. Rev. Lett. **56**, 2533 (1986).

[11] L. Banyai and S. W. Koch, Phys. Rev. Lett. **57**, 2722 (1986).

[12] S. Mukamel and E. Hanamura, Phys. Rev. A **33**, 1099 (1986).

[13] M. Ueta, H. Kanzaki, K. Kobayashi, Y. Toyozawa, and E. Hanamura, *Excitonic Processes in Solids* (Springer-Verlag, Heidelberg, 1986), p. 137.

[14] R. K. Jain and R. C. Lind, J. Opt. Soc. Am. **73**, 647 (1983).

[15] P. Roussignol. D. Ricard, K. C. Rustagi, and C. Flytzanis, Opt. Commun. **55**, 143 (1985).

[16] S. S. Yao, C. Karaguleff, A. Gabel, F. Fortenberry, C. T. Seaton, and G. I. Stegeman, Appl. Phys. Lett. **46**, 801 (1985).